AN ELECTROCHEMICAL INVESTIGATION OF THE STRUCTURE OF COPPER(II) COMPLEXES OF SCHIFF BASE LIGANDS DERIVED FROM SALICYLALDEHYDE AND SUBSTITUTED ANILINES

Maddalena CORSINI[a1], Emanuela GRIGIOTTI[a2], Franco LASCHI[a3], Piero ZANELLO[a4,*], John BURGESS[b], John FAWCETT[b1,*] and Syeda R. GILANI[b2]

[a] *Dipartimento di Chimica dell'Università di Siena, Via Aldo Moro, 53100 Siena, Italy; e-mail: [1] mcorsini@unisi.it, [2] grigiotti@unisi.it, [3] laschi@unisi.it, [4] zanello@unisi.it*

[b] *Department of Chemistry, University of Leicester, Leicester LE1 7RH, U.K.; e-mail: [1] jxf@leicester.ac.uk, [2] rubinagilani@yahoo.com*

Received May 9, 2003
Accepted July 2, 2003

Dedicated to Professor Sergio Roffia on the occasion of his retirement.

An electrochemical investigation has been carried out on a series of Schiff base copper(II) complexes derived from salicylaldehyde and substituted anilines in the attempt to correlate the solid-state geometry of the CuN_2O_2 core, which is conditioned by the steric encumbrance of the different peripheral substituents, and the corresponding solution structures as inferred from either the distinctive features of the Cu(II)/Cu(I) reduction or the EPR characteristics of the original complexes. Even if a good agreement is expected between the extent of chemical reversibility of the reduction process and the tetrahedral distortion of the complexes, it has been found, that in reality, the chemical reversibility of the reduction process also holds for nominally planar complexes in that they are sufficient flexible to pass from planar to tetrahedral arrangements upon addition of one electron. The relative location of the Cu(II)/Cu(I) formal electrode potentials appears more pertinent in that the higher is the distortion the less negative is the potential value.

Keywords: Copper(II) complexes; Crystal structure determination; Electrochemistry; EPR spectroscopy; Schiff base complexes; Imines; Salene complexes.

In a previous paper, some of us reported the crystal structure of the copper(II) complexes **3**–**6** with Schiff base ligands derived from salicylaldehyde and substituted anilines[1] (Scheme 1). The crystal structure of the unsubstituted complex **7** is known[2]. We report here the electrochemical and EPR characterisation of the complete series together with the crystal structure of complex **1**.

Ligand substituents	*Cu(II) complexes*
R^1 = H, R^2 = R^3 = Me	**1**
R^1 = CF_3, R^2 = R^3 = H	**2**
R^1 = F, R^2 = R^3 = H	**3**
R^1 = H, R^2 = R^3 = CF_3	**4**
R^1 = OCF_3, R^2 = R^3 = H	**5**
R^1 = Me, R^2 = H, R^3 = F	**6**
R^1 = R^2 = R^3 = H	**7**

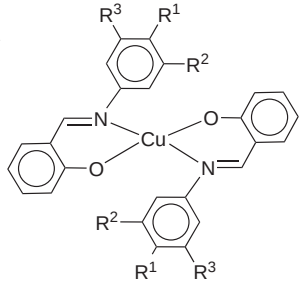

SCHEME 1

It is well known that tetrahedrally distorted Cu(II) complexes can favour reduction to the corresponding, usually tetrahedral, Cu(I) derivatives, whereas square-planar Cu(II) complexes can give access to the corresponding, rigidly planar, Cu(III) derivatives[3,4]. Since some of the present complexes exhibit in the solid state geometric features intermediate between square-planar and tetrahedral (namely, **1** and **4**), we decided to investigate their redox behaviour together with its EPR characteristics, in order to better define their structural flexibility in solution.

EXPERIMENTAL

Complexes **3**–**6** and **7** were prepared as previously described[1,2]. Complex **1** was prepared by adding a solution of copper(II) acetate (1 mmol) in a 50% ethanol–water mixture (10 ml) to a hot solution of salicylaldehyde (1 mmol) and 3,5-dimethylaniline (1 mmol) in ethanol (20 ml). Precipitation occured immediately and the reaction mixture was cooled; the resulting product was filtered and washed with ethanol. Yield 75%; m.p. 228 °C. For $C_{30}H_{28}CuN_2O_2$ (512.1) calculated: 49.5% C, 2.21% H, 3.85% N; found: 49.74% C, 2.15% H, 3.56% N. The same method was used to prepare compound **2** from 4-(trifluoromethyl)aniline.

Crystal Structure

Crystal data: $C_{30}H_{28}CuN_2O_2$, (**1**) M = 512.08, monoclinic, space group $C2/c$, a = 21.573(1) Å, b = 15.067(1) Å, c = 17.204(1) Å, β = 118.53(1) Å, U = 4913.1(4) Å^3, Z = 8, μ = 0.92 mm^{-1}, λ(MoKα) = 0.71073 Å, F(000) = 2136, D_c = 1.385 Mg m^{-3}. Data collected at 150 K. $R_1\{F^2 > 2\sigma(F^2)\}$ = 0.0343, wR_2 (all data) = 0.100; GOF = 1.045.

Crystals were grown from $CHCl_3$, a brown plate crystal was used for data collection with approximate dimensions 0.23 × 0.9 × 0.03 mm. Data were collected on a Bruker APEX 2000 CCD diffractometer using graphite-monochromated MoKα radiation (λ = 0.7107 Å). The data were corrected for Lorentz and polarisation effects and an empirical absorption correction applied. Structure solution by Patterson methods and structure refinement on F^2 employed SHELXTL version 6.10 (ref.[5]). Hydrogen atoms were included in calculated positions (C–H = 0.96 Å) riding on the bonded atom with isotropic displacement parameters set

to 1.5 U_{eq}(C) for methyl H atoms and 1.2 U_{eq}(C) for all other H atoms. All non-H atoms were refined with anisotropic displacement parameters.

CCDC 212894 contains the supplementary crystallographic data for this paper. These data can be obtained free of charge *via* www.ccdc.cam.ac.uk/conts/retrieving.html (or from the Cambridge Crystallographic Data Centre, 12, Union Road, Cambridge, CB2 1EZ, UK; fax: +44 1223 336033; or deposit@ccdc.cam.ac.uk).

Electrochemistry and EPR Measurements

Materials and apparatus for electrochemistry and joint EPR spectroscopy have been described elsewhere[6]. Potential values are referred to the saturated calomel electrode (SCE). Under the present experimental conditions, the one-electron oxidation of ferrocene occurs at +0.39 V.

RESULTS AND DISCUSSION

Crystal structure of **1**. As illustrated in Fig. 1, there are two unique molecules in the unit cell with very different molecular geometries.

The 3,5-dimethylphenyl rings of the ligands bonded to Cu1 are located parallel and on the same side of the molecule in very close proximity, such that C8 and C8′ are separated by only 3.09 Å. By contrast, the rings of the ligands bonded to Cu2 are on opposite sides of the molecule and approximately orthogonal. The Cu atoms of both molecules are located on two-fold axes and, as a consequence, the asymmetric unit consists of two half-molecules. Despite the difference in overall molecular geometry, the geometry at the metal atom is similar and approximately intermediate between square-planar and tetrahedral. The interplanar angles Cu1–N1–O1 with Cu1–N1′–O1′ and Cu2–O2–N2 with Cu2–N2′–O2′ are 42.0 and 48.3°, respectively. The most significant structure parameters are collected in Table I.

Electrochemistry

As a typical example of the cyclic voltammetric behaviour exhibited by the present copper(II) complexes, Fig. 2 shows the cyclic voltammetric profile of **5** in dichloromethane solution.

The cathodic sweep points out the presence of a reduction process displaying features of chemical reversibility, which is in turn followed by a minor process at very negative potential values. In the anodic sweep, a first oxidation process of intensity roughly comparable to the first reduction and also having some features of chemical reversibility is closely accompanied by further minor processes.

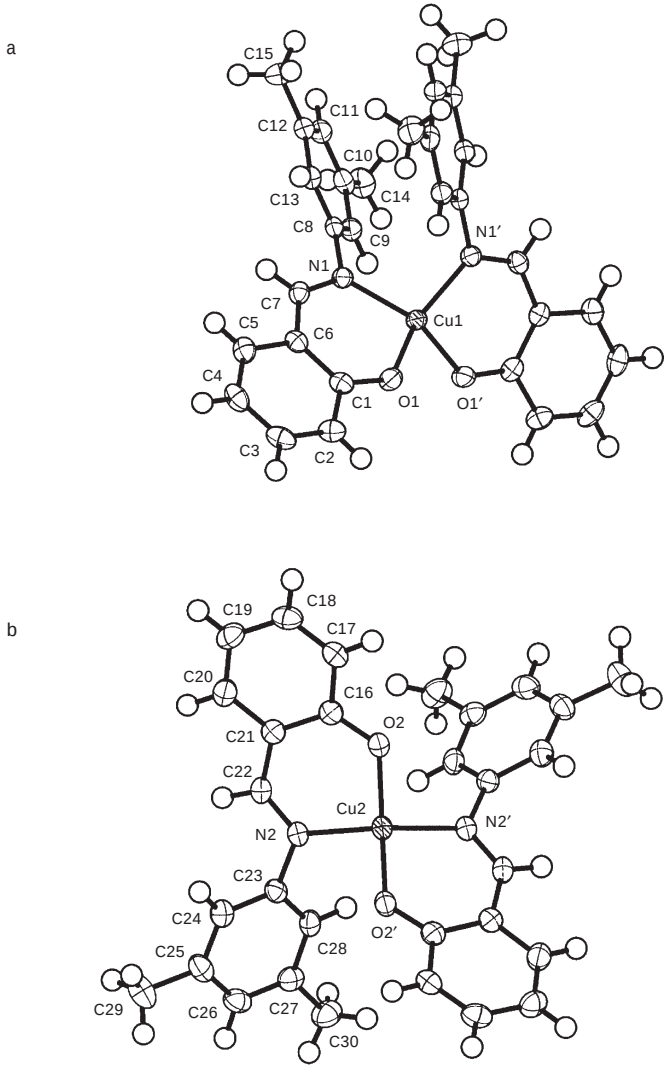

FIG. 1

Molecular structures of the unique molecules showing the atom label schemes and 50% displacement probability ellipsoids. Hydrogen atoms are shown as spheres of arbitrary radius. The Cu atoms are both located on a two-fold axis, primed atoms are generated by symmetry ($1 - x$, y, $1½ - z$)

TABLE I
Selected bond lengths (in Å) and angles (in °) for **1**

Cu(1)–O(1)	1.8822(14)
Cu(1)–N(1)	1.9689(17)
Cu(2)–O(2)	1.8990(15)
Cu(2)–N(2)	1.9622(17)
O(1)#1–Cu(1)–O(1)	87.35(9)
O(1)–Cu(1)–N(1)#1	148.78(7)
O(1)–Cu(1)–N(1)	93.90(7)
N(1)#1–Cu(1)–N(1)	100.68(10)
O(2)#1–Cu(2)–O(2)	141.58(10)
O(2)–Cu(2)–N(2)#1	95.52(7)
O(2)–Cu(2)–N(2)	94.63(7)
N(2)#1–Cu(2)–N(2)	148.81(10)

Symmetry transformations used to generate equivalent atoms: #1 1 – *x*, *y*, 1½ – *z*.

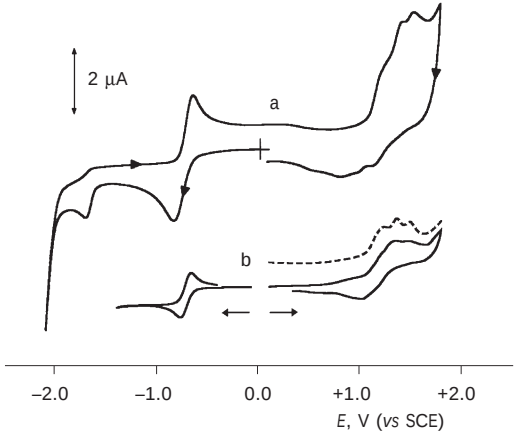

FIG. 2
Cyclic (——) and Osteryoung square-wave (– – –) voltammograms recorded at a platinum electrode in a CH_2Cl_2 solution of **5** (1.4×10^{-3} mol dm^{-3}). $[NBu_4][PF_6]$ (0.2 mol dm^{-3}) supporting electrolyte. Scan rates: cyclic voltammetry 0.2 V s^{-1} (a); 0.05 V s^{-1} (b). Osteryoung square-wave voltammetry 0.1 V s^{-1}

Controlled potential coulometric tests in correspondence to the first reduction step (E_w = –1.0 V) consumed one electron per molecule and the resulting solution afforded cyclic voltammetric profiles quite complementary to the original ones, thus testifying to the chemical reversibility of the Cu(II)/ Cu(I) reduction ([**5**]/[**5**]$^-$) also in the long times of macroelectrolysis.

Analysis[7] of the cyclic voltammetric responses of the reduction process with scan rates varying from 0.02 to 2.00 V s^{-1} shows that: (i) the current function $i_{pc}\,v^{-1/2}$ decreases by about 20% for a tenfold increase in the scan rate; (ii) the current ratio i_{pa}/i_{pc} maintains constantly equal to 1; (iii) the peak-to-peak separation, ΔE_p, progressively increases from 105 to 343 mV. Such a trend is diagnostic for a simple quasireversible one-electron process, the marked quasireversibility of which suggests that a significant structural strain must be overcome on passing from planar Cu(II)-[**5**] to more or less tetrahedral Cu(I)-[**5**]$^-$ (refs[3,4]).

Based on the relative peak heights, we also assume that the first oxidation might involve a one-electron process, naively attributable to the Cu(II)/ Cu(III) oxidation, [**5**]/[**5**]$^+$, which, being not completely stable, likely generates byproducts responsible for the coupled oxidations. As briefly alluded to above, the access to Cu(III) suggests that the complex, at least in the cyclic voltammetric time scale, can maintain the planar geometry upon one-electron removal.

More difficult is to assign the second cathodic process in that its peak height is significantly lower than that of the Cu(II)/Cu(I) process, both at low and high scan rates, thus contrasting the straightforward Cu(I)/Cu(0) assignment. Such an assignment is further ruled out by the absence of the typical anodic stripping peak, which usually accompanies the irreversible Cu(I)/Cu(0) reduction[4]. In view of the minor importance of such a process we do not venture any assignment.

Since the above voltammetric picture essentially holds for all the present Cu(II) complexes, except for complexes **1** and **6** which are relatively unstable in the Cu(I) oxidation state even on the cyclic voltammetric time scale, it is deduced that, in solution, complexes **2**–**5** and **7** are rather structurally flexible to shuttle from planar to tetrahedral upon one-electron removal/ addition, even if the quasireversibility of the pertinent processes means that the relevant reorganization barriers are rather high.

The formal electrode potentials for the most significant redox changes exhibited by all the complexes studied are compiled in Table II.

Detecting a univocal thermodynamic trend that might favour the access to Cu(II) or Cu(III) is complicated by the fact that the structural factors couple with the inductive effects of the aniline substituents. What is specu-

latively evident from the structural viewpoint is that complex **7**, in agreement with its planarity not perturbed by the presence of aniline substituents, is one of the most difficult to reduce and easiest to oxidise, whereas complex **4**, due to the tetrahedral distortion in the solid state imposed by the sterically encumbering substituents, is the easiest to reduce and the most difficult to oxidise. In the latter case, however, it is clear that the electron-withdrawing CF_3 substituents also contribute to favour the electron addition. By contrast, the related complex **1**, which also has some degree of tetrahedral distortion in the solid state, is notably hard to reduce because of the electron-donating effect of the CH_3 substituents.

As shown, Table II also reports the overall electronic effects played by the aniline substituents as Hammett σ constants[8]. A plot of $E^{\circ\prime}$(Cu(II)/Cu(I)) *vs* Σσ gives a correlation coefficient of 0.91, thus indicating a roughly linear dependence of the electrode potentials from the inductive effects of the substituents. As far as the Cu(II)/Cu(III) process is concerned, we naively assume that its substantial chemical irreversibility points out that even in the less tetrahedrally distorted complexes there is an intrinsic difficulty to maintain the planar geometry upon electron removal.

We finally point out that the HOMO-LUMO separation for all the Cu(II) complexes, as calculated from the difference between the formal electrode potentials of the first oxidation and the first reduction, is within 1.8–1.9 eV.

TABLE II
Formal electrode potentials (V *vs* SCE; t = 25 °C), peak-to-peak separations (mV) and current ratios for the redox changes exhibited by the Cu(II) complexes under study in CH_2Cl_2 solution

Complex	$E^{\circ\prime}_{Cu(III)/Cu(II)}$	ΔE_p [a]	i_{pc}/i_{pa} [a]	$E^{\circ\prime}_{Cu(II)/Cu(I)}$	ΔE_p [a]	i_{pa}/i_{pc} [a]	Σσ
1	+1.01	300	0.4	–0.84	240	0.7	–0.14
2	+1.17	110	[b]	–0.70	150	0.9	0.54
3	+1.13	160	0.8	–0.74	116	1.0	0.06
4	+1.18	160	[b]	–0.68	175	1.0	0.86
5	+1.19[c]	[b]	[b]	–0.72	105	1.0	0.35
6	+1.0[d]	[b]	[b]	–0.77	194	0.6	0.17
7	+1.09	130	[b]	–0.80	115	0.9	0

[a] Measured at 0.05 V s^{-1}; [b] difficult to evaluate because the partial overlapping of the second anodic process makes the anodic peak poorly resolved (see the text); [c] from Osteryoung square-wave voltammetry; [d] peak potential for irreversible processes.

EPR Spectroscopy

As a typical example of the EPR features of the complexes under study, Fig. 3 shows the X-band spectra of complex **1** in CH_2Cl_2 solution both at liquid nitrogen (T = 100 K) and at ambient (T = 298 K) temperatures.

In frozen solution, the anisotropic Cu(II) line shape (spin Hamiltonian S = 1/2) displays a well-resolved rhombic structure ($\boldsymbol{g}_l >> \boldsymbol{g}_m >> \boldsymbol{g}_h \neq \boldsymbol{g}_{electron}$ = 2.0023), the large value of the $\delta\boldsymbol{g}_{l/h} = \boldsymbol{g}_l - \boldsymbol{g}_h$ parameter (0.226(6)) testifying to the strong Cu(II) λ spin–orbit coupling[9,10]. The three anisotropic regions display different SAI magnetic interactions. The low-field absorption is well resolved in the typical Cu(II) hyperfine (hpf) splitting (^{63}Cu: I = 3/2, natural abundance = 69.1%; ^{65}Cu: I = 3/2, natural abundance = 30.1%). The two narrow higher-field hpf bands are closely spaced and present partial resolution of the underlying Cu(II) hpf or N super-hyperfine (shpf) contributions (^{14}N: I = 1, natural abundance > 99%), $\Delta H_{m,h} \geq a_{m,h}$(Cu, N). Raising the temperature under frozen conditions improves the high-field hpf resolution of the $\boldsymbol{g}_m$ region, thus allowing a reliable estimation of the a_m(Cu) values.

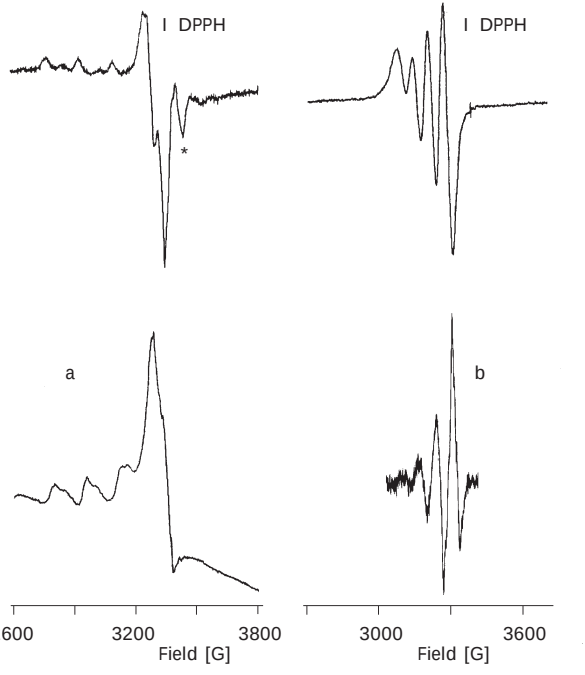

FIG. 3

X-Band EPR spectra of **1** in CH_2Cl_2 solution. T = 100 K (a); T = 298 K (b). Top: first derivative; bottom: second derivative; (non SI unit used 1G = 10^{-4} T)

Based on the $g_{||}/A_{||}$ parameter[10], the actual frozen solution anisotropic features support the presence of some tetrahedral distortion of the CuN_2O_2 core of complex **1**, and hence are in agreement with the solid-state X-ray structure (see above).

At the glassy-fluid transition (T = 178 K), the rhombic spectrum collapses in a well hpf resolved isotropic line shape. The overall ΔH_{iso} is strongly dependent upon temperature, significantly narrowing at higher temperatures due to effective shortening of the S = 1/2 electron spin relaxation times[9]. As expected, the line width and a_{iso}(Cu) of the isotropic signals exhibit dependence from both the magnetic field H and m_I, in that the anisotropy induced by distortion is not completely averaged in liquid solution[9,10]. In this connection, Fig. 3b shows the room temperature spectrum of complex **1**. The second derivative line shape displays a partial resolution of the nitrogen shpf structure in the high-field Cu(II) hpf m_I = 3/2 line. A broad quintuplet appears as a consequence of the magnetic interaction of the S = 1/2 unpaired electron with the two magnetically equivalent nitrogen nuclei of the ligand in an approximately square-planar coordination (distorted D_{4h} local symmetry). It is noted that complexes **2**, **3**, **5** and **7** bearing the less encumbering substituents in meta positions afford isomerism in solution.

Finally, the solid-state EPR spectrum of complex **1** at room temperature exhibits a strongly unsymmetrical line shape with a well resolved narrow axial structure ($g_{\perp} > g_{||} \neq g_{electron}$), Fig. 4.

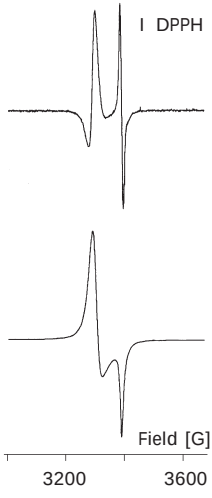

FIG. 4
Solid-state X-band EPR spectra of **1** at room temperature. Bottom: first derivative; top: second derivative

TABLE III

Temperature-dependent X-band EPR parameters of the Cu(II) complexes under study in different experimental conditions (standard deviations from fitting procedure are in parentheses)

Complex		g_l	g_m	g_h	$\langle g \rangle$	$\delta g_{l/h}$	g_{iso}	a_l	a_m	a_h	$\langle a \rangle$	a_{iso}
1	(297K)[a]	2.150(5)	2.150(5)	2.058(5)	2.119(5)	0.092(5)	–	$\leq\Delta H_l$	$\leq\Delta H_m$	$\leq\Delta H_h$	$\leq\langle\Delta H\rangle$	–
	(106K)[a]	2.146(5)	2.146(5)	2.058(5)	2.116(5)	0.088(5)	–	$\leq\Delta H_l$	$\leq\Delta H_m$	$\leq\Delta H_h$	$\leq\langle\Delta H\rangle$	–
	(105K)[b]	2.246(10)	2.076(6)	2.020(6)	2.114(10)	0.226(10)	2.116(5)	168(8)	13(6)	$\leq\Delta H_h$	$\leq\langle\Delta H\rangle$	63(8) 12(8)
2*	(297K)[a]	2.215(10)	2.071(6)	2.037(6)	2.108(10)	0.178(10)	–	$\leq\Delta H_l$	$\leq\Delta H_m$	$\leq\Delta H_h$	$\leq\langle\Delta H\rangle$	–
	(107K)[a]	2.250(10)	2.071(6)	2.030(6)	2.117(10)	0.220(10)	–	$\leq\Delta H_l$	$\leq\Delta H_m$	$\leq\Delta H_h$	$\leq\langle\Delta H\rangle$	–
	(105K)[b]	2.289(10)	2.041(5)	2.016(5)	2.115(10)	0.273(10)	2.119(5)	165(8)	12(5)	$\leq\Delta H_h$	$\leq\langle\Delta H\rangle$	71(5) 11(5)
3*	(297K)[a]	2.204(6)	2.093(6)	2.025(6)	2.107(6)	0.179(6)	–	$\leq\Delta H_l$	$\leq\Delta H_m$	$\leq\Delta H_h$	$\leq\langle\Delta H\rangle$	–
	(108K)[a]	2.199(8)	2.087(6)	2.030(6)	2.103(8)	0.176(8)	–	$\leq\Delta H_l$	$\leq\Delta H_m$	$\leq\Delta H_h$	$\leq\langle\Delta H\rangle$	–
	(100K)[b]	2.243(8)	2.062(8)	2.014(5)	2.106(8)	0.229(8)	2.126(6)	160(6)	15(6)	$\leq\Delta H_h$	$\leq\langle\Delta H\rangle$	68(6) 13(6)
4	(297K)[a]	[c]	2.064(6)	2.026(6)	[c]	[c]	–	$\leq\Delta H_l$	$\leq\Delta H_m$	$\leq\Delta H_h$	$\leq\langle\Delta H\rangle$	–
	(106K)[a]	2.325(10)	2.060(6)	2.023(10)	2.136(10)	0.302(10)	–	$\leq\Delta H_l$	$\leq\Delta H_m$	$\leq\Delta H_h$	$\leq\langle\Delta H\rangle$	–
	(103K)[b]	2.210(10)	2.064(6)	2.026(6)	2.100(10)	0.184(10)	2.116(8)	186(6)	$\leq\Delta H_m$	$\leq\Delta H_h$	$\leq\langle\Delta H\rangle$	73(6) 13(6)
5*	(297K)[a]	2.232(10)	2.068(6)	2.034(6)	2.111(10)	0.198(10)	–	$\leq\Delta H_l$	$\leq\Delta H_m$	$\leq\Delta H_h$	$\leq\langle\Delta H\rangle$	–
	(106K)[a]	2.255(10)	2.071(6)	2.034(6)	2.120(10)	0.221(10)	–	$\leq\Delta H_l$	$\leq\Delta H_m$	$\leq\Delta H_h$	$\leq\langle\Delta H\rangle$	–
	(105K)[b]	2.246(10)	2.056(6)	2.014(6)	2.105(10)	0.232(10)	2.107(5)	165(8)	13(6)	14(6)	64(6)	69(5) 14(5)
6	(297K)[a]	2.258(10)	2.077(5)	2.037(5)	2.124(10)	0.221(10)	–	$\leq\Delta H_l$	$\leq\Delta H_m$	$\leq\Delta H_h$	$\leq\langle\Delta H\rangle$	–
	(104K)[a]	2.224(10)	2.083(5)	2.040(5)	2.116(10)	0.184(10)	–	$\leq\Delta H_l$	$\leq\Delta H_m$	$\leq\Delta H_h$	$\leq\langle\Delta H\rangle$	–
	(103K)[b]	2.237(10)	2.066(6)	2.012(6)	2.105(10)	0.225(10)	2.119(5)	162(10)	12(6)	$\leq\Delta H_h$	$\leq\langle\Delta H\rangle$	66(5) 13(5)
7*	(297K)[a]	2.250(10)	2.052(6)	2.036(6)	2.113(10)	0.214(10)	–	$\leq\Delta H_l$	$\leq\Delta H_m$	$\leq\Delta H_h$	$\leq\langle\Delta H\rangle$	–
	(105K)[a]	2.176(10)	2.079(6)	2.039(6)	2.098(10)	0.137(10)	–	$\leq\Delta H_l$	$\leq\Delta H_m$	$\leq\Delta H_h$	$\leq\langle\Delta H\rangle$	–
	(115K)[b]	2.237(8)	2.051(5)	2.001(5)	2.096(10)	0.236(10)	2.114(5)	165(6)	12(5)	18(5)	65(5)	68(5) 13(5)

* Most abundant isomer in fluid solution at room temperature. [a] Solid state; [b] CH_2Cl_2 solution; [c] undetectable signal. $\langle g \rangle = 1/3(g_l + g_m + g_h)$; $\langle a \rangle = 1/3(a_l + a_m + a_h)$.

Neither Cu(II) hpf nor N shpf structure are evident in the two anisotropic regions, due to strong JSS magnetic interaction (JSS = super-exchange interaction Hamiltonian)[9]. Small variations in the anisotropic spectral parameters (g_i, ΔH_i) occur on decreasing the temperature, suggesting that thermal contributions do not alter the magnetic nature of the complex (or its molecular geometry). Accordingly, no $\Delta m_s = 2$ mid-field transitions were detected, suggesting that no dimeric species form[9,10].

The best-fit spectral parameters, calculated according to literature procedures[11], are collected in Table III, together with those of all complexes under study.

In solution, the paramagnetic features of all the Cu(II) complexes are basically similar, but, based on the variation of the $\delta g_{l/h}$ parameter, it is argued that in frozen condition the geometrical departure from the strictly planar structure follows the order **2** > **7** > **5** > **1** ≈ **3**. This result partially conflicts with the solid-state findings (which assign tetrahedral distortion to **1** and **4**), but is in agreement with the chemical reversibility of the relative Cu(II)/Cu(I) reductions. In reality, based on the electrochemical data, also complex **4** in solution at ambient temperature would present some tetrahedral distortion.

In conclusion, the data show that in addition to the expected structure differences induced by different phases (solid state *vs* solution), the molecular geometry of the present four-coordinate copper(II) complexes also have a temperature dependence.

P. Zanello gratefully acknowledges the financial support from the University of Siena (PAR 2001).

REFERENCES

1. Burgess J., Fawcett J., Palma V., Gilani S. R.: *Acta Crystallogr., Sect. C: Cryst. Struct. Commun.* **2001**, *57*, 277.
2. Baker E. N., Hall D., Waters T. N.: *J. Chem. Soc. A* **1966**, 680.
3. Zanello P.: *Comments Inorg. Chem.* **1988**, *8*, 45.
4. P. Zanello in: *Stereochemistry of Organometallic and Inorganic Compounds* (I. Bernal, Ed.), Vol. 4, p. 181. Elsevier, Amsterdam 1990.
5. *SHELXTL, An Integrated System for Solving, Refining and Displaying Crystal Structures*. Version 6.10. Bruker Analytical X-Ray Systems, Madison (WI) 1997.
6. Zanello P., Laschi F., Fontani M., Mealli C., Ienco A., Tang K., Jin X., Li L.: *J. Chem. Soc., Dalton Trans.* **1999**, 965.
7. Brown E. R., Sandifer J. R. in: *Physical Methods of Chemistry, Electrochemical Methods* (B. W. Rossiter and J. F. Hamilton, Eds), Vol. 2, Chap. 4. Wiley, New York 1986.
8. Hansch C., Leo A., Taft R. W.: *Chem. Rev. (Washington, D. C.)* **1991**, *91*, 165.

9. a) Mabbs F. E., Collison D.: *Studies in Inorganic Chemistry*, Vol. 16. Elsevier, Amsterdam 1992; b) Drago R. S.: *Physical Methods for Chemist*. Saunders College Publishing, New York 1992.
10. a) Bencini A., Gatteschi D.: *Transition Metal Chemistry: A Series of Advances*, Vol. 8. Marcel Dekker, New York 1982; b) Sakaguchi U., Addison A. W: *J. Chem. Soc., Dalton Trans.* **1979**, 600; c) Barbaro P., Bianchini C., Capannesi G., DiLuca L., Laschi F., Petroni D., Salvadori P. A., Vacca A., Vizza F.: *J. Chem. Soc., Dalton Trans.* **2000**, 2393; d) Subramanian P. S., Suresh E., Srinivas D.: *Inorg. Chem.* **2000**, *39*, 2053; e) Losada J., del Peso I., Beyer L.: *Inorg. Chim. Acta* **2001**, *321*, 107; f) Pilbrow J. R.: *Transition Ion Electron Paramagnetic Resonance*. Claredon Press, Oxford 1990.
11. a) Lozos J. P., Hoffman B. M., Franz C. G.: *Quantum Chemistry Program Exchange* **1974**, *11*, 265; b) Della Lunga G.: *ESRMGR Simulation Program*. Department of Chemistry, University of Siena, Siena 1994.